

Communication

# Investigation of Optical Cavity Dynamics with Raman and Ytterbium-Doped Gain Media Integration

Efrain Mejia-Beltran \* and Oscar J. Ballesteros-Llanos

Centro de Investigaciones en Óptica, A.C., Loma del Bosque 115, León 37150, Mexico

\* Correspondence: emejiab@cio.mx

**Abstract:** This study delves into a comprehensive examination of an optical cavity system that integrates Raman and Yb-doped gain media, with a focus on understanding their interactions. The research implies a characterization of each gain medium within the cavity while subjecting them to diverse co-pumping conditions with the other. When the Raman-lasing cavity is co-pumped by exciting the Yb-doped section, the resulting composite laser exhibits significant threshold reductions and there is an optimal co-pumping regime that enhances energy transfer from pump to Stokes. As for the complementary cavity, where the Yb-doped gain is influenced by the co-pumped Raman gain, at moderate pump powers a light-controlling-light behavior phenomenon arises. Within this regime, the 1064 nm signal suppresses the Yb-generated 1115 nm signal, suggesting potential applications in intracavity optical modulation. For higher pump levels, a cooperative effect emerges whereby both lasers mutually enhance each other. Minor variations in the primary 974 nm pump power, even by just a few milliwatts, result in significant capabilities for switching or modulating the Stokes signal. Under these conditions of mutual enhancement, the hybrid optical system validates notable improvements regarding energy transfer efficiency and threshold reduction. This research provides valuable insights into the intricate dynamics of optical cavity systems and reveals promising avenues for applications in advanced optical modulation technologies.

**Keywords:** Raman fiber lasers; Ytterbium-doped fiber lasers; stimulated Raman scattering; amplified spontaneous emission



**Citation:** Mejia-Beltran, E.; Ballesteros-Llanos, O.J. Investigation of Optical Cavity Dynamics with Raman and Ytterbium-Doped Gain Media Integration. *Photonics* **2023**, *10*, 1148. <https://doi.org/10.3390/photonics10101148>

Received: 31 August 2023  
Revised: 26 September 2023  
Accepted: 3 October 2023  
Published: 12 October 2023



**Copyright:** © 2023 by the authors. Licensee MDPI, Basel, Switzerland. This article is an open access article distributed under the terms and conditions of the Creative Commons Attribution (CC BY) license (<https://creativecommons.org/licenses/by/4.0/>).

## 1. Introduction

Over the past two decades, research efforts in the domains of Raman fiber lasers (RFLs) and Ytterbium-doped fiber lasers (YbDFLs) have experienced a substantial surge in activity. This heightened interest is primarily attributable to their exceptional performance characteristics and their potential applications across a wide spectrum of research and industrial fields [1–3]. It is worth noting that both the RFLs and the YbDFLs operate within a shared wavelength range, spanning from just below 1000 nm to 1200 nm [4–6]. This specific emission range is defined by the radiative properties of  $\text{Yb}^{3+}$  ions embedded within the glass of the optical fibers [7,8]. As previously established, the emissions spanning from 976 to 1200 nm in ytterbium-doped fibers (YbDFs) play a crucial role in facilitating the generation of the lowest Raman-generated Stokes components within 1064 nm of pumped silica fibers. Specifically, these emissions manifest at 1115 nm and 1175 nm [9]. In a parallel line of inquiry, which underpins the complementary hypothesis of our research, these YbDF emissions may also offer amplification capabilities to a Raman fiber laser (RFL). Indeed, the convergence of these two distinct types of fiber lasers, one based on a rare earth-doped media and the other relying on Raman scattering, in a cooperative operating mode forms the core of the investigations reported herein.

The genesis of combining multiple laser systems within a shared cavity can be traced back to the generation of Raman Stokes signals during the production of high peak powers, reaching approximately 10 kW, in Ytterbium-doped fiber lasers, as elucidated in [10]. These

YbDFLs typically featured relatively short fiber cavity lengths, often on the order of a few tens of meters. Consequently, the generation of Raman Stokes signals within such compact cavities, especially in a continuous wave (CW) mode, was deemed improbable, as it typically necessitates cavity extensions on the order of hundreds of meters when dealing with CW pumps operating at watt-level power. To the best of our knowledge, the inaugural proposal of a CW hybrid system can be traced back to the work reported by us in Ref. [9]. In this pioneering experiment, a 1064-nanometer pump laser concurrently excited a composite cavity comprising a 1.27 m YbDF spliced to a 350 m silica fiber. Subsequent research endeavors further advanced this concept, resulting in notable enhancements in efficiency, as documented in [11–13]. In the contemporary landscape, numerous reports have emerged that extend the concept into amplifier and pulsed laser systems, with a substantial escalation in power levels [14,15]. These contributions have played a role in augmenting traditional laser systems, be they solely RFLs or YbDFLs. Furthermore, researchers have explored alternative rare-earth elements in various regions, as exemplified in Ref. [16]. However, to our knowledge, none have delved into the intricate dynamics of independently and interdependently pumping each gain medium within the shared cavity, which constitutes the primary focus and objective of the research presented herein.

In this study, we initiated the experimentation by pumping a Raman fiber laser cavity containing an un-pumped segment of YbDF. This YbDF segment was then subjected to co-pumping using a 974 nm laser diode. Subsequently, we directed our attention to the YbDFL cavity, which encompassed an extended silica fiber segment that was similarly un-pumped and co-pumped at 1064 nm. Through this experimental setup, we systematically characterized the system under both operating conditions, meticulously evaluating the advantages and disadvantages inherent in each configuration within the composite laser cavity.

## 2. Experiments

After several tries, we determined that the experimental setup illustrated in Figure 1 was the most suitable for testing our hypotheses. In this, a single-spatial mode continuous-wave (CW) 1064 nm fiber laser from IPG-Photonics® was collimated and passed through an optical isolator (OI) towards a 10× focusing lens that coupled into arm a of a wavelength division multiplexer (WDM). The WDM transmitted 61% of the 1064 nm light through arm c, while transmitting only 3% of it through arm d; the complimentary 36% was the insertion loss and it was polarization-independent. The pumping arm c was spliced to a fiber Bragg grating (FBG)-based hybrid cavity of the nested type consisting of two close-to 95% reflectance for the first Stokes (1115 nm) and a pair of ~87% for the second Stokes (1176 nm). The composed gain medium included a 4.7 km (quasi-single mode, 6.5-micron core diameter) TrueWave® silica fiber for the Raman gain; it was spliced to a 6-micron core (single mode) 1.5 m length 1.25% concentration YBDF as the complimentary gain medium. The YbDF was pumped at the opposite end of the cavity by a 974 nm laser diode (LD) that provided up to 250 mW, as depicted in the upper left of the figure.

Each choice of fiber length was made with careful consideration, taking into account two key factors. First, the wavelength-division multiplexer (WDM) had a power handling limit of 3 watts (W) for optical signals. Second, the 974-nanometer (nm) laser diode could provide a maximum power output of approximately 250 milliwatts (mW). Given these constraints, our goal was to generate two Stokes components within the Raman cavity by directing 61% of the maximum pump power, which was 2.5 W at the WDM entrance, resulting in a maximum available power of 1.3 W for this purpose. To achieve this, we needed an extensive length of silica fiber, specifically the 4.7 km True-Wave fiber. Interestingly, the Ytterbium-Doped Fiber (YbDF) did not introduce additional fiber losses. On the contrary, it functioned as a weak amplifier, exhibiting slight absorption at 1064 nm while amplifying wavelengths at 1117 nm and 1175 nm [9]. In practical terms, it could be considered transparent for our purposes. To enable the generation of the two Stokes components, it was imperative to construct a high-Q (high quality factor) cavity. We

accomplished this by splicing high reflectance fiber Bragg gratings (FBGs), as will be elaborated upon later. One of the most challenging aspects of this process was optimizing the length of the YbDF. It needed to provide sufficient gain at 1117 nm to compensate for the substantial losses within the cavity. Each kilometer of silica fiber introduced approximately 1 dB loss, totaling 4.7 dB in a single pass. The high-Q nature of the cavity played a crucial role in this regard. Our optimization process involved a series of trial-and-error steps. We began with the shortest YbDF length of around 10 cm and progressively increased it to 20 cm, 40 cm, and so on. We continued until we reached the longest available length of 1.5 m, at which point the cavity operated satisfactorily at 1115 nm. It is important to note that, in the case of a quasi-two-level distributed gain medium like a YbDF, longer lengths of the medium favor the gain of longer wavelengths. Additionally, the increase in temperature, which occurred due to the power levels involved in our experiments, reinforced the shifting of the spectrum towards the infrared wavelengths.

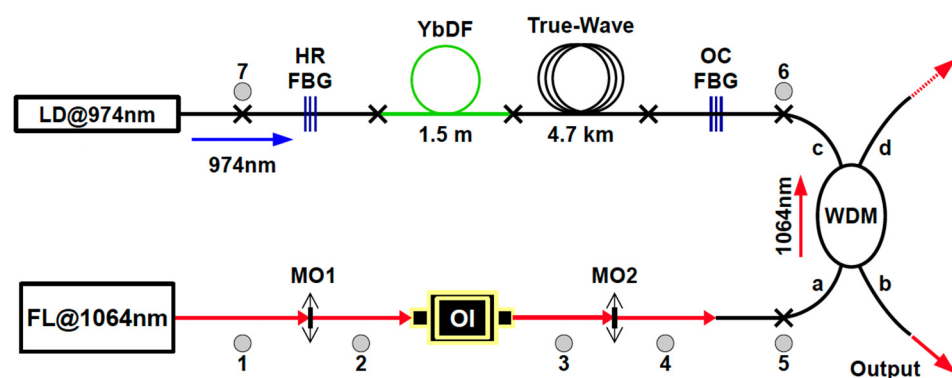


**Figure 1.** Experimental setup: “OI” refers to the optical isolator; “MOs” represent 10× microscope objectives; “HR” stands for high reflecting; and “OC” denotes output coupler. Pumping of the Ytterbium-Doped Fiber (YbDF) cavity with a 974 nm signal occurs at point seven, while the 1064 nm Raman pumping takes place at point six, in a counterpropagating direction.

The methodology for the experiments started by first characterizing the composed cavity with 1064 nm pumping alone and then, also pumping alone, with 974 nm. After this, we pumped for each type of gain while simultaneously pumping the other one. The signals generated were monitored at arm b of the WDM, whose transmittances of signals coming from arm care were ~50% of 1115 nm, ~7% of backscattered 1064 nm, and ~17% of the second Stokes (~55% went to arm a and was blocked by the OI).

### 3. Results

As previously outlined, the characterizations were essentially divided into two distinct approaches, as expounded upon immediately below.

#### 3.1. The Co-Pumped Raman Cavity

When coupling pump powers to the Raman gain within the cavity at point six of Figure 1, spanning a power range from 0 W to 1.1 W, we conducted measurements to determine the first Stokes powers delivered at the output arm of the WDM. The resulting data are graphically represented by the black curves in Figure 2. Note that the Stokes commenced its generation at approximately 0.35 W. It is worth noting that there is a noticeable inflection point at around 0.55 W. This inflection point signifies an energy transfer from the first Stokes component to the second Stokes component, as illustrated by the black plot in Figure 3. This plot illustrates the power levels corresponding to the delivery of approximately 17% of the backward-generated second Stokes signal.

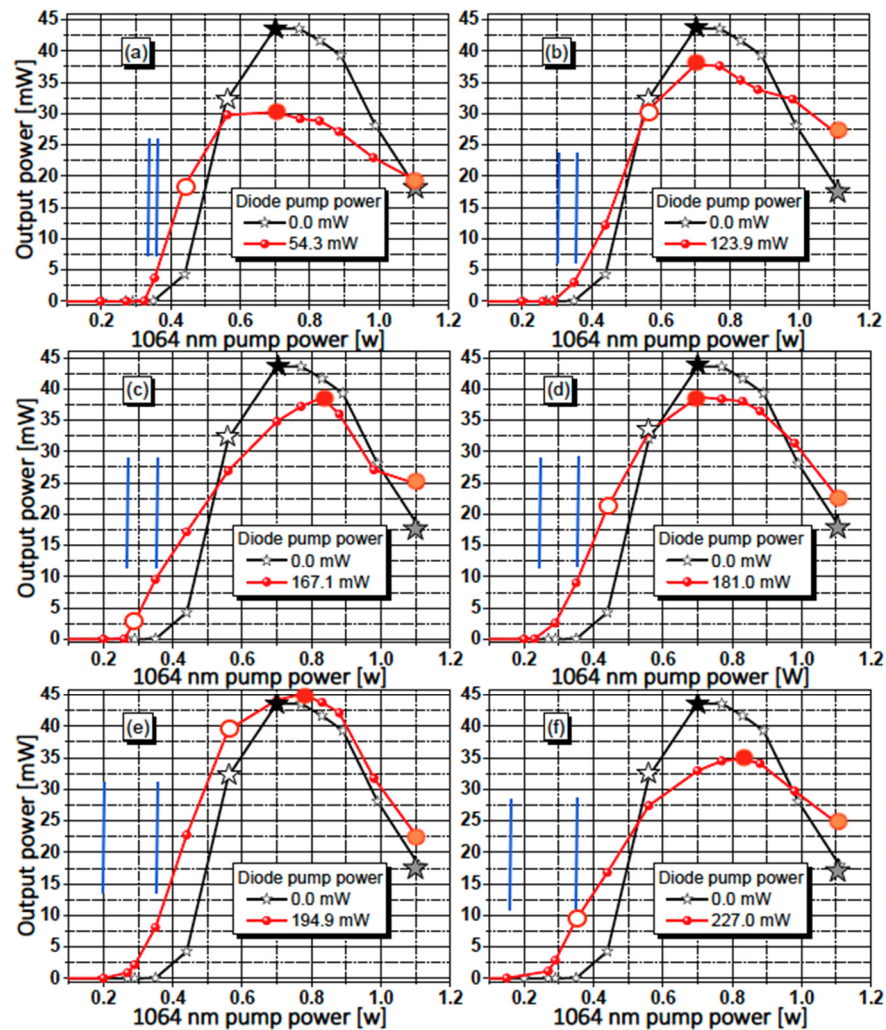


**Figure 2.** First Stokes signal vs. pump power. In all the insets, the black curves marked with stars represent the pure Raman laser. The red curves marked with spheres represent the system operating in a hybrid mode, where multiple levels of the 974 nm signal co-pump the Yb-doped section with the following powers: (a) 54.3 mW, (b) 123.9 mW, (c) 167.1 mW, (d) 181 mW, (e) 194.9 mW, and (f) 227 nm. The blue parallel lines are indicative of alterations in threshold magnitude. The prominent stars, differentiated by their white, black, and gray hues, symbolize the initiation of the energy transfer, the pinnacle of the Stokes emission, and the corresponding Stokes output at maximum pump, respectively. A parallel interpretation pertains to the sizable red circular markers within the curves.

Please note that the first Stokes signal reaches its maximum intensity when the pump power exceeds 0.7 W, resulting in an output of approximately 44 mW. This corresponds to the point at which the energy transfer to the second Stokes signal becomes dominant. As the pump power reaches its maximum of 1.1 W, the intensity of the first Stokes signal is reduced to around 40% of its peak value, allowing the second Stokes signal to absorb the majority of the available energy.

The red plots in Figures 2 and 3 correspond to the co-pumping of the YbDF in the opposite direction. Notice the distinct changes in Stokes signal generation for various pump levels of the 974 nm signal. For instance, in Figure 2a, there is a subtle threshold reduction for the first Stokes generation when co-pumping with 54.3 mW. This trend of lowering the threshold persists as these levels increase, becoming more pronounced when co-pumping with 124 mW, which decreases the threshold from 0.35 W down to 0.3 W (Figure 2b). With 167 mW, the threshold decreases to 0.27 W (Figure 2c); with 181 mW, it decreases down

to 0.24 W (Figure 2d); with 195 mW, it decreases down to 0.2 W (Figure 2e); and, with 227 mW, it decreases down to 0.1 W (Figure 2f). In summary, there is a 71% reduction in the threshold, decreasing from 0.35 W to 0.1 W with the total available power of 227 mW.

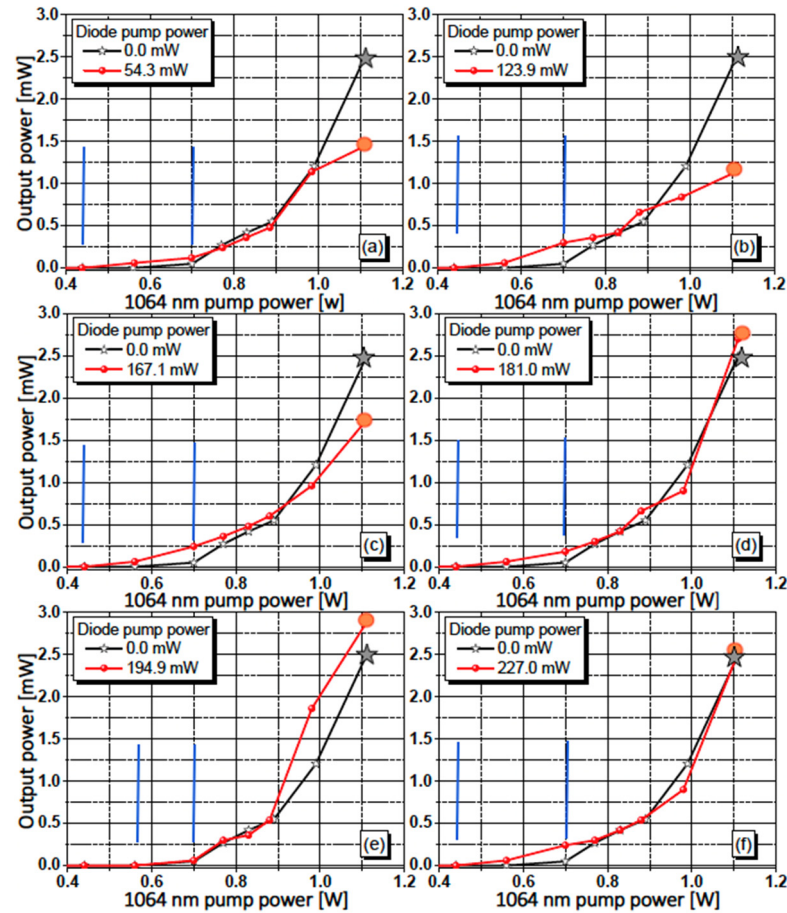


**Figure 3.** Second Stokes vs. pump power. The black curves marked with stars represent the pure Raman laser. The red curves marked with spheres correspond to the hybrid system, where multiple levels of the 974 nm signal co-pump the Yb-doped section as follows: (a) 54.3 mW, (b) 123.9 mW, (c) 167.1 mW, (d) 181 mW, (e) 194.9 mW, and (f) 227 nm.

When analyzing the changes in the energy transfer induced by co-pumping, let us compare the red plots with the black ones in all the insets of Figures 2 and 3. The first Stokes signal (Figure 2), as mentioned earlier, begins generating earlier with co-pumping. However, it also depletes earlier, and in most cases, except for Figure 2e, its curve reaches a lower peak intensity. This indicates an earlier initiation of the energy transfer to the next Stokes component. It is important to note that the second Stokes signal (Figure 3), except in the case of Figure 3e, is also generated earlier with co-pumping. However, it is at this co-pump level that, above the threshold, it is not only generated more efficiently but also notably reaches higher power. In summary, these results suggest that both Stokes components generate earlier when assisted by the pumped Yb ions, leading to an increase in the overall system efficiency. Additionally, regarding Figures 2e and 3e, it appears that there exists an optimal co-pump power level. This level not only enhances the efficiency of the generated Stokes but also maximizes the energy transfer from the pump to both Stokes signals.

### 3.2. The Co-Pumped Yb-Doped Cavity

When pumping the Yb-doped gain of the cavity above the threshold with 0.148 W, the cavity emitted at 1115 nm, as shown in Figure 4a. Note that the intensity was normalized

to one. When turning off the 974 nm while pumping the Raman gain medium below the threshold (0.2 W), the cavity did not oscillate and only the backscattered pump was present, as displayed in Figure 4b. By turning on again the 974 nm pump, we obtained the “combined” behavior depicted in Figure 4c.

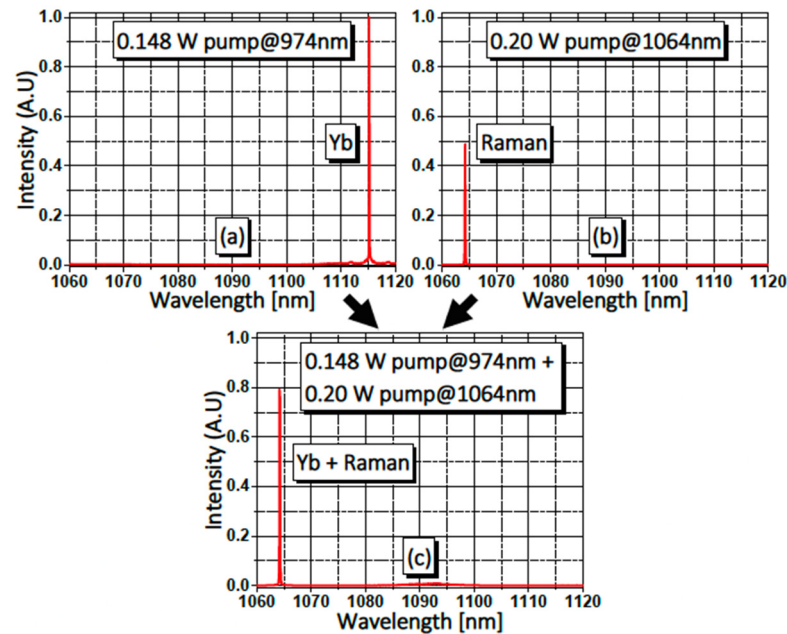


**Figure 4.** (a) Pumping as a pure Yb<sup>3+</sup> cavity with 148 mW; (b) pumping as a pure Raman cavity with 200 mW (below threshold); and (c) combined operation.

It is worth noting that the laser line at 1115 nm originating from Yb becomes completely suppressed by the 1064 nm signal, which experiences amplification (from 0.5 to 0.8). This outcome holds significant promise for potential applications in light-controlling-light-based modulators [17,18]. In this scenario, the 1064 nm signal effectively governs and manipulates the energy that would otherwise produce the 1115 nm signal. This modulating mechanism’s underlying phenomenon can be explained by the fact that the inverted population amplifies the 1064 nm signal rather than the 1115 nm signal. This preference for the 1064 nm signal is due to its proximity to the peak amplification of the Yb<sup>3+</sup> ions, which is typically centered around 1040 nm [19].

By further increasing the pump power of the 1064 nm laser by approximately 30% (0.29 W), while still remaining below the pure Raman oscillation threshold of 0.35 W, the system transitions into what we term as the “composite” operational state, as visually represented in Figure 5c. In this configuration, the 1115 nm component generated by the Yb ions within the cavity continues to be partially suppressed by the amplified 1064 nm signal. Consequently, in a light-controlling-light system, the controlling signal (1064 nm) exceeds its anticipated level because the 1115 nm signal is not completely suppressed. We speculate that the amplified 1064 nm signal contributes to an increase in spontaneous Raman scattering (RS). This RS, combined with the portion of amplified spontaneous emission (ASE) produced by the Yb ions that coincides with the FBGs, may trigger stimulated Raman scattering (SRS) and/or the 1115 nm Yb signal within the high-Q cavity. Under these conditions, it becomes challenging to definitively determine whether it operates as a RFL, a YbDFL, or a hybrid of both. Hence, it is imperative to conduct further experiments, which fall beyond the scope of this study, to gain a comprehensive understanding and characterize this behavior.

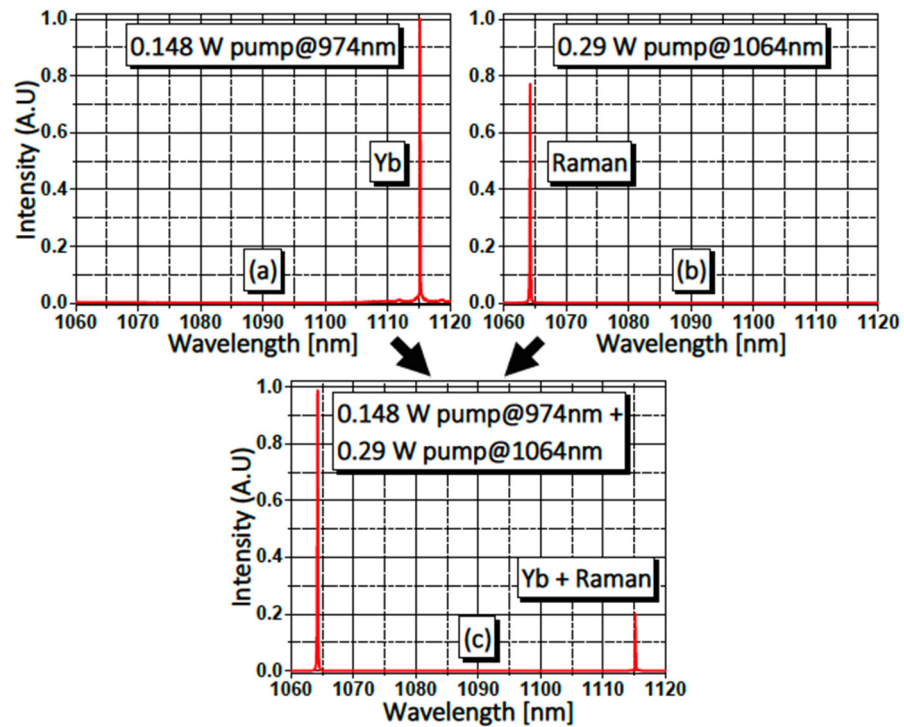


**Figure 5.** (a) Pumping as a pure Yb<sup>3+</sup> cavity with 148 mW; (b) pumping as a pure Raman cavity with 290 mW (just below threshold); and (c) combined operation.

The complete characterization of the cavity operating as a YbDFL, with no 1064 nm signal (0W), is depicted by curve (a) in Figure 6. The lasing threshold for this configuration was approximately 138 mW of the 974 nm signal. Notably, at the maximum pump power of 227 mW, the laser delivered an output of approximately 9.6 mW. Furthermore, Figure 6 includes additional curves that represent the laser behavior for various 1064 nm co-pump signal levels, specifically: (b) 0.7 W, (c) 0.9 W, and (d) 1 W.

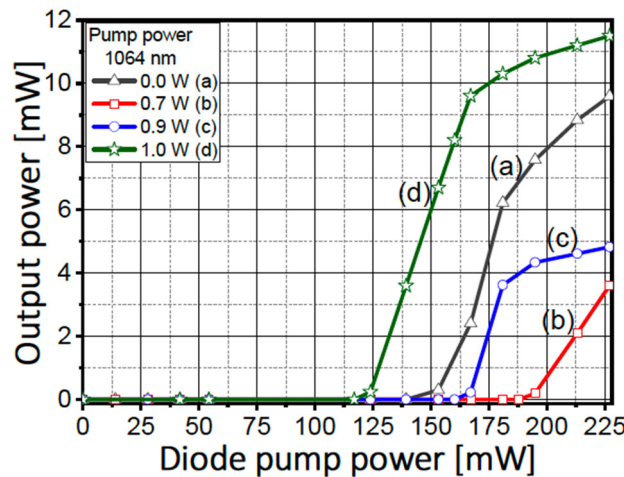


**Figure 6.** Power delivery of YbDFL vs. pump power in the low co-pump power regime. Each curve represents a different co-pumping scenario: (a) without 1064 nm co-pumping; (b) co-pumped with 0.7 W; (c) co-pumped with 0.9 W; and (d) co-pumped with 1 W.

Please note that, despite the co-pump powers of 0.7 W and 0.9 W being higher than the pure Raman threshold of 0.35 W, both the threshold and efficiency of the YbFL are notably affected. It is at the 1.0 W co-pump power level that the combined synergy becomes significant. At this point, the threshold drops significantly from 160 mW to 115 mW, marking

a substantial 28% reduction. Moreover, the efficiency improves dramatically, increasing by 230%, even though the pump power only increased by 10%. This demonstrates a remarkable improvement in both the threshold and the efficiency under the influence of this co-pumping synergy.

In Figure 7, we present similar characterizations corresponding to co-pump powers equal to or greater than the well-established combination of both laser systems sharing the same cavity. Curve (d) corresponds to the optimal performance seen in Figure 6. When we add an additional 0.2 W of co-pumping power, representing a 20% increase, the threshold is significantly reduced by 58% (from 115 mW to 48 mW). Simultaneously, the efficiency experiences a remarkable 330% increase, climbing from 11.5 mW to 38 mW. It is important to highlight that, for this level and the subsequent ones, there is a steep slope just above the threshold. In other words, small variations, on the order of a few milliwatts, in the power range from 40 to 48 mW, result in a significant increase in the delivered signal. For instance, with a 2.5 W co-pump (curve h), an increase of approximately 12 mW leads to a jump in the delivered signal from zero to 98 mW. Once again, in a light-controlling-light system, a relatively small 974 nm signal can effectively control, switch, or modulate a much larger first Stokes signal that is an order of magnitude stronger. This behavior also indicates an early initiation of energy transfer from the first to the second Stokes component. This is evident as the curve drastically bends, leading to a first Stokes depletion for the diode pump powers around 180 mW and the co-pump powers of 1.5 W, 2.0 W, and 2.5 W (curves f, g, and h in Figure 7).

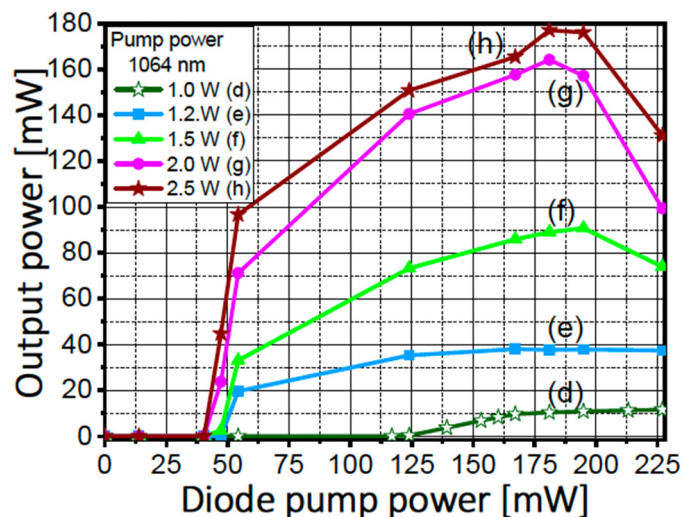


**Figure 7.** Power delivery of YbDFL vs. pump power in the high co-pump power regime: (d) Co-pumped with 1 W (same as Figure 6); (e) co-pumped with 1.2 W; (f) co-pumped with 1.5 W; (g) co-pumped with 2 W; and (h) co-pumped with 2.5 W.

#### 4. General Discussions

In the contemporary exploration of Ytterbium (Yb)-enhanced Raman systems, both gain media components are conjoined within a singular cavity, sharing a common pump source. This innovative configuration has unveiled considerable promise in advancing the efficiency and augmenting the capabilities of laser and amplifier technologies. Nevertheless, it is imperative to underscore that these advancements do not inherently imbue the system with additional functionalities, as both elements are contingent on the utilization of a shared power source. In contrast, when Yb ions are provided with their independent pump source, they manifest increased activity and autonomy, consequently engendering novel functionalities. This paradigm shift towards the independent control of the light within the hybrid cavity unveils a vast spectrum of possibilities. In this discourse, we propose classical applications that find relevance in well-established domains of laser technology, encompassing pulse generation, pulse shaping, light switching, and optical modulation.

From a phenomenological perspective, a minor signal, exemplified here as a 974-nanometer wavelength emission, whether originating from a physically interconnected source or an external one, exerts a profound influence on the intracavity signal. This phenomenon bears promising implications for optical sensors and optical communication systems alike. Of paramount significance is the ability to manipulate the core properties, rendering the cavity opaque, semi-transparent, entirely transparent, or even capable of amplification, through the utilization of a compact electronically driven optical co-pump source. This capability empowers the generation of pulses that need not adhere to uniform temporal spacing. Furthermore, electronic control can dictate the generation of pulses within a great diversity of shapes. While this approach holds immense potential, it remains imperative to conduct comprehensive studies that address numerous pertinent questions that naturally arise, including aspects related to signal purity, noise, chaos, and other relevant parameters. In conclusion, we assert that this proof of concept opens the door to a multitude of intriguing research avenues and opportunities for advancement within the realms of laser engineering and the related scientific disciplines.

## 5. Conclusions

We conclude that our study underscores the exciting prospects of harnessing the synergistic potential between distinct gain media within optical cavities. Specifically, in the Raman process, co-pumping within the Yb-doped cavity showcased significant reductions in threshold values and enhancements in efficiency. In this, optimal enhancements consisted of the right adjustment of the co-pumping levels. Conversely, within the Yb-doped enhanced cavity, we observed captivating light-controlling-light phenomena, opening the doors to advanced modulation applications like mode-locking or Q-switching. In this configuration, we observed substantial mutual enhancements that synergistically reduced thresholds and improved efficiency. This research underscores the promise of innovative optical cavity designs that are adaptable for a wide range of applications in photonics, telecommunications, and beyond, presenting novel opportunities for controlling and modulating light.

**Author Contributions:** Conceptualization, E.M.-B.; Data curation, O.J.B.-L.; Funding acquisition, E.M.-B.; Investigation, O.J.B.-L.; Methodology, E.M.-B. and O.J.B.-L.; Supervision, E.M.-B.; Visualization, O.J.B.-L.; Writing—original draft, E.M.-B.; Writing—review and editing, E.M.-B. and O.J.B.-L. All authors have read and agreed to the published version of the manuscript.

**Funding:** This research was funded by CONACYT-Mexico, under grant reference CB-2011-01/166740 and scholarship No. 339086 and the APC was funded by Centro de Investigaciones en Optica, A.C.

**Institutional Review Board Statement:** Not applicable.

**Informed Consent Statement:** Not applicable.

**Data Availability Statement:** No new data were created or analyzed in this study.

**Conflicts of Interest:** The authors declare no conflict of interest.

## References

1. Bromage, J. Raman Amplification for Fiber Communications Systems. *J. Lightw. Technol.* **2004**, *22*, 79–93. [[CrossRef](#)]
2. Georgiev, D.; Gapontsev, V.P.; Dronov, A.G.; Vyatkin, M.Y.; Rulkov, A.B.; Popov, S.V.; Taylor, J.R. Watts-level frequency doubling of a narrow line linearly polarized Raman fiber laser to 589 nm. *Opt. Exp.* **2005**, *13*, 6772–6776. [[CrossRef](#)] [[PubMed](#)]
3. Feng, Y.; Taylor, L.; Bonaccini Calia, D. 25 W Raman-fiber-amplifier-based 589 nm laser for laser guide star. *Opt. Exp.* **2009**, *17*, 19021–19026. [[CrossRef](#)] [[PubMed](#)]
4. Frazão, O.; Correia, C.; Rocco Giraldi, M.T.M.; Marques, M.B.; MSalgado, H.; Martinez, M.A.G.; Costa, J.C.A.; Barbero, A.P.; Baptista, J.M. Stimulated Raman scattering and its applications in optical communications and optical sensors. *Open Opt. J.* **2009**, *3*, 1–11. [[CrossRef](#)]
5. Dianov, E.M. Raman fiber amplifiers. *Adv. Fiber Opt.* **2000**, *4083*. [[CrossRef](#)]
6. Kurkov, A.S.; Paramonov, V.M.; Medvedkov, O.I. Ytterbium fiber laser emitting at 1160 nm. *Laser Phys. Lett.* **2006**, *3*, 503–506. [[CrossRef](#)]

7. Pask, H.M.; Carman, R.J.; Hanna, D.C.; Tropper, A.C.; Mackechnie, C.J.; Barber, P.R.; Dawes, J.M. Ytterbium-Doped Silica Fiber Lasers: Versatile Sources for the 1–1.2  $\mu\text{m}$  Region. *IEEE J. Sel. Topics Quantum Electron.* **1996**, *1*, 2–13. [[CrossRef](#)]
8. Kurkov, A.S. Oscillation spectral range of Yb-doped fiber lasers. *Laser Phys. Lett.* **2007**, *4*, 93–102. [[CrossRef](#)]
9. de la Cruz-May, L.; Mejía, E.B. Raman fiber laser improvement by using Yb<sup>3+</sup>-doped fiber. *Laser Phys.* **2009**, *19*, 1017–1020. [[CrossRef](#)]
10. Chernikov, S.V.; Zhu, Y.; Taylor, J.R.; Gapontsev, V.P. Supercontinuum self-Q-switched ytterbium fiber laser. *Opt. Lett.* **1997**, *22*, 298–300. [[CrossRef](#)] [[PubMed](#)]
11. Nicholson, J.W.; Taunay, T.; Monberg, E.; DiMarcello, F.; Li, Y.; Ng, J. All-in-one 1236 nm Yb/Raman fiber laser. *Fiber Lasers IX Technol. Syst. Appl.* **2012**, 8237, 823733. [[CrossRef](#)]
12. Chen, Y.; Xiao, H.; Xu, J.; Leng, J.; Zhou, P. Laser diode-pumped dual-cavity high-power fiber laser emitting at 1150 nm employing hybrid gain. *Appl. Opt.* **2016**, *55*, 3824–3828. [[CrossRef](#)] [[PubMed](#)]
13. Oscar; Ballesteros-Llanos, J.; Mejía-Beltrán, E.; Juárez-Hernández, M. Hybrid (Raman-Ytterbium) ring-cavity fabry-perot-filtered fiber laser. *OFT* **2021**, *67*, 102693. [[CrossRef](#)]
14. Qi, T.; Li, D.; Wang, Z.; Wang, L.; Yu, W.; Yan, P.; Gong, M.; Xiao, Q. 6.85 kW Ytterbium-Raman Fiber Amplifier Based on Adjustable Raman Threshold Method. *J. Lightw. Technol.* **2022**, *12*, 3907–3915. [[CrossRef](#)]
15. Liu, X.; Hao, W.; Yang, Z.; Tang, Y. High-peak-power random Yb-fiber laser with intracavity Raman-frequency comb generation. *High Power Laser Sci. Eng.* **2023**, *11*, E11. [[CrossRef](#)]
16. Anashkina, E.A.; Andrianov, A.V. Numerical Study of Efficient Tm-Doped Zinc-Tellurite Fiber Lasers at 2300 nm. *Fibers* **2023**, *11*, 57. [[CrossRef](#)]
17. Mejía-Beltrán, E.; Velázquez, T.D. Talavera. Red (632.8-nm) attenuation by a copropagating 1175-nm signal in Tm<sup>3+</sup>-doped optical Fibers. *Opt. Eng.* **2007**, *46*, 105001. [[CrossRef](#)]
18. Mejía, E.; Pinto, V. Optically controlled loss in an optical fiber. *Opt. Lett.* **2009**, *34*, 2796–2798. [[CrossRef](#)] [[PubMed](#)]
19. Mejía, E.B.; de la Cruz-May, L. Spectral changes produced by an adjustable intra-cavity Fabry–Perot interferometer inside an ytterbium-doped fiber laser. *Laser Phys.* **2015**, *25*, 095101. [[CrossRef](#)]

**Disclaimer/Publisher’s Note:** The statements, opinions and data contained in all publications are solely those of the individual author(s) and contributor(s) and not of MDPI and/or the editor(s). MDPI and/or the editor(s) disclaim responsibility for any injury to people or property resulting from any ideas, methods, instructions or products referred to in the content.